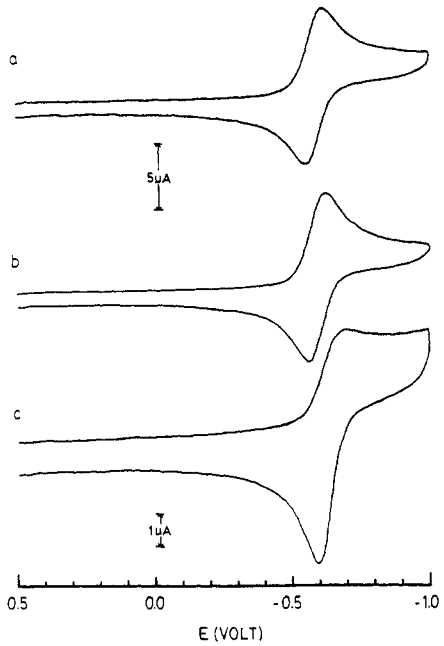

Figure 7. Cyclic voltammograms of $[Re(dmpe)_2Cl_2]^+$ in aqueous solution: (a) 0.1 M SDS/0.1 M TEAP, [Re] = 1.51 mM; (b) 0.1 M SDS/0.1 M (TEA)Cl, [Re] = 1.50 mM; (c) 0.1 M SDS/0.1 M NaCl, [Re] = 1.61 mM. The scan rate is 100 mV/s.

a reduction in Faradaic current for all complexes; in fact, the current is reduced to such an extent that reliable voltammetric information can be obtained only for $[Re(dmpe)_2Cl_2]^+$ and $[Re(dmpe)_2Br_2]^+$, which exhibit peak potentials of -0.608 and -0.548 V, respectively. The replacement of TEAP by tetraethylammonium chloride has no significant effect on voltammograms obtained in 0.1 M SDS (Figure 7), and thus the effect induced by NaCl clearly results from the replacement of the tetraethylammonium cation by the sodium cation. This effect on the electrochemistry in SDS micellar solution is attributed to changes induced in the micellar environment by the cations from the supporting electrolyte; the cmc values of 0.1 M SDS in the presence of 0.1 M NaCl and 0.1 M TEAP are 1.5 and 0.1 mM, respectively. The 15-fold decrease in cmc reflects a greater tendency for surfactant aggregation in the presence of the tetraethylammonium cation. The larger tetraethylammonium cation presumably ion-pairs more effectively with the dodecyl sulfate anion than does the smaller, more hydrophilic, sodium cation. The effect of this tetraethylammonium ion-pairing on the structure of the SDS micelles should be similar to the effect engendered by the incorporation of heptanol,[37] i.e., increased distances between the anionic SDS head groups, which result in a tighter, more closely packed, micellar environment. The more tightly packed TEAP/SDS micelles apparently allow for more efficient electron transfer between the electrode and solubilized complexes than do the more loosely packed Na/SDS micelles.

Acknowledgment. Financial support by the National Institutes of Health, Grant No. HL21276 and CA42179 (E.D.), and the Department of Energy, Grant No. DE-FG02-86ER60487 (W. R.H.), is gratefully acknowledged. J.R.K. also wishes to thank Dr. Hendrik Emons of Karl-Marx-University Leipzig and Dr. Jim Sullivan of Argonne National Laboratory for many helpful discussions.

---

(37) Russell, J. C.; Whitten, D. G. *J. Am. Chem. Soc.* **1982**, *104*, 5937-5942.

Contribution from the Biomedical Chemistry Research Center, Department of Chemistry, University of Cincinnati,
Cincinnati, Ohio 45221, Department of Chemistry, Rosary College, River Forest, Illinois 60305,
and Chemistry Division, Argonne National Laboratory, Argonne, Illinois 60439

Structural and Kinetic Investigations of a Tc(III)/Tc(II) Redox Couple. X-ray Crystal Structures of *trans*-$[Tc^{II}(DPPE)_2Cl_2]$ and *trans*-$[Tc^{III}(DPPE)_2Cl_2]NO_3{\cdot}HNO_3$, Where DPPE = 1,2-Bis(diphenylphosphino)ethane[1]

Karen Libson,[2] Mary Noon Doyle,[2] Rudy W. Thomas,[2] Theodore Nelesnik,[2] Mary Woods,[3]
James C. Sullivan,[4] R. C. Elder,[2] and Edward Deutsch*,[2]

Received January 11, 1988

The components of a reversible Tc(III/II) redox couple have been characterized by single-crystal X-ray analysis. The Tc(II) complex *trans*-$[Tc(DPPE)_2Cl_2]$ (fw = 966.67) crystallizes in the monoclinic space group $P2_1/a$ with $a = 17.821$ (4) Å, $b = 11.187$ (2) Å, $c = 23.572$ (4) Å, $\beta = 103.55$ (1)°, and $Z = 4$; 4945 observed reflections were refined to a weighted R factor of 0.029. The Tc(III) salt *trans*-$[Tc(DPPE)_2Cl_2]NO_3{\cdot}HNO_3$ (fw = 1091.69) crystallizes in the triclinic space group $P\bar{1}$ with $a = 10.083$ (2) Å, $b = 11.119$ (4) Å, $c = 12.767$ (1) Å, $\alpha = 71.80$ (1)°, $\beta = 73.68$ (1)°, $\gamma = 69.35$ (1)°, and $Z = 1$; 5697 observed reflections were refined to a weighted R factor of 0.035. Oxidation of the Tc(II) complex to the Tc(III) form causes a shortening of the Tc-Cl bond by 0.105 (2) Å, consistent with the ionic nature of this interaction. Conversely, oxidation from Tc(II) to Tc(III) causes a lengthening of the Tc-P bond by 0.072 (2) Å, consistent with the domination of this interaction by π-back-bonding from Tc to P. The magnitudes of these bond length changes are used to predict the inner-sphere reorganizational barrier to electron transfer of the *trans*-$[Tc(DPPE)_2Cl_2]^{+/0}$ couple to be only ca. 2.6 kcal/mol. Preliminary kinetic studies in nonaqueous media confirm that *trans*-$[Tc^{II}(DPPE)_2X_2]$ (X = Cl, Br) complexes are facile electron-transfer partners for a variety of 1-equiv oxidants. The rate of reduction of $[(en)_2Co(S(CH_2C_6H_4CH_3)CH_2CH_2NH_2)]^{3+}$ by *trans*-$[Tc^{II}(DPPE)_2Cl_2]$ in acetonitrile (25 °C; $\mu = 0.10$ M) is 3.0 (7) × 10^4 M^{-1} s^{-1}.

Introduction

Redox-active technetium complexes are of considerable interest for nuclear medicine applications.[5,6] Technetium(III/II) complexes of the general formula *trans*-$[TcD_2X_2]^{+/0}$ (where D represents a chelating bis(tertiary phosphine or arsine) ligand and X represents a halide or pseudohalide ligand) are of special interest since some of the Tc(III) cations are taken up by the heart[7-10]

---

[1] Abstracted in part from: (a) Libson, K. Ph.D. Thesis, University of Cincinnati, 1981. (b) Noon, M. Ph.D. Thesis, University of Cincinnati, 1984.

[2] University of Cincinnati.

[3] Rosary College.

[4] Argonne National Laboratory.

[5] Deutsch, E.; Libson, K.; Jurisson, S.; Lindoy, L. F. *Prog. Inorg. Chem.* **1983**, *30*, 75.

[6] Deutsch, E.; Libson, K. *Comments Inorg. Chem.* **1984**, *3*, 83.

[7] Deutsch, E.; Bushong, W.; Glavan, K. A.; Elder, R. C.; Sodd, V. J.; Scholz, K. L.; Fortman, D. L.; Lukes, S. J. *Science (Washington, D.C.)* **1981**, *214*, 85.

0020-1669/88/1327-3614$01.50/0 © 1988 American Chemical Society

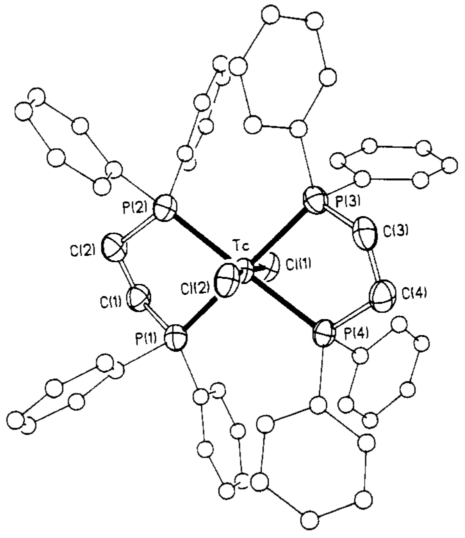

Figure 1. Perspective drawing of the Tc(II) cation *trans*-[Tc(DPPE)$_2$Cl$_2$]$^+$, showing 50% probability ellipsoids and spheres. Hydrogen atoms are omitted for clarity.

and some of the neutral Tc(II) species cross the blood–brain barrier.[11,12] Moreover, reduction of the Tc(III) cation *trans*-[Tc(DMPE)$_2$Cl$_2$]$^+$ (where DMPE represents 1,2-bis(dimethylphosphino)ethane) to the neutral Tc(II) form has been shown to occur in vivo.[13] The structural and kinetic studies reported herein have been undertaken in order to better define the inorganic chemistry that underlies these biological processes.[5,6,14]

Table I. Fractional Atomic Positional Parameters[a,b] for *trans*-[Tc^{II}(DPPE)$_2$Cl$_2$]

atom	*x*	*y*	*z*
Tc	0.29556 (2)	0.44320 (2)	0.25808 (1)
Cl(1)	0.33032 (5)	0.62965 (7)	0.21982 (4)
Cl(2)	0.25078 (5)	0.26783 (7)	0.30197 (3)
P(1)	0.42991 (5)	0.45387 (8)	0.31312 (4)
P(2)	0.35926 (5)	0.33961 (8)	0.19099 (4)
P(3)	0.16522 (5)	0.45030 (8)	0.19862 (4)
P(4)	0.23207 (5)	0.55064 (8)	0.32215 (4)
C(1)	0.4871 (2)	0.4626 (3)	0.2573 (1)
C(2)	0.4654 (2)	0.3576 (3)	0.2163 (1)
C(3)	0.1017 (2)	0.4409 (3)	0.2494 (1)
C(4)	0.1257 (2)	0.5269 (3)	0.3002 (1)
C(11)	0.4629 (2)	0.5828 (3)	0.3604 (1)
C(12)	0.4673 (2)	0.5756 (3)	0.4200 (2)
C(13)	0.4870 (2)	0.6742 (4)	0.4556 (2)
C(14)	0.5038 (2)	0.7809 (4)	0.4334 (2)
C(15)	0.4998 (2)	0.7893 (3)	0.3744 (2)
C(16)	0.4801 (2)	0.6927 (3)	0.3385 (1)
C(21)	0.4811 (2)	0.3325 (3)	0.3581 (1)
C(22)	0.5604 (2)	0.3396 (4)	0.3826 (2)
C(23)	0.5995 (2)	0.2453 (5)	0.4146 (2)
C(24)	0.5613 (3)	0.1455 (4)	0.4236 (2)
C(25)	0.4841 (3)	0.1362 (3)	0.4001 (2)
C(26)	0.4445 (2)	0.2288 (4)	0.3675 (2)
C(31)	0.3571 (2)	0.1787 (3)	0.1751 (1)
C(32)	0.3804 (2)	0.1355 (3)	0.1263 (2)
C(33)	0.3847 (3)	0.0155 (4)	0.1164 (2)
C(34)	0.3653 (3)	0.0646 (4)	0.1536 (2)
C(35)	0.3439 (3)	0.0255 (3)	0.2024 (2)
C(36)	0.3401 (3)	0.0961 (3)	0.2128 (2)
C(41)	0.3367 (2)	0.4033 (3)	0.1170 (2)
C(42)	0.3764 (2)	0.4999 (4)	0.1027 (2)
C(43)	0.3547 (3)	0.5518 (4)	0.0487 (2)
C(44)	0.2936 (3)	0.5087 (5)	0.0018 (2)
C(45)	0.2532 (3)	0.4112 (4)	0.0210 (2)
C(46)	0.2744 (2)	0.3591 (3)	0.0755 (2)
C(51)	0.1333 (2)	0.5852 (3)	0.1554 (2)
C(52)	0.0672 (3)	0.6484 (4)	0.1583 (2)
C(53)	0.0474 (3)	0.7410 (5)	0.1254 (2)
C(54)	0.0895 (4)	0.7878 (4)	0.0874 (2)
C(55)	0.1536 (3)	0.7246 (5)	0.0834 (2)
C(56)	0.1765 (3)	0.6245 (4)	0.1167 (2)
C(61)	0.1240 (2)	0.3316 (3)	0.1460 (2)
C(62)	0.1458 (2)	0.2145 (3)	0.1604 (2)
C(63)	0.1149 (3)	0.1219 (4)	0.1224 (2)
C(64)	0.0633 (3)	0.1467 (5)	0.0711 (2)
C(65)	0.0427 (3)	0.2603 (5)	0.0568 (2)
C(66)	0.0724 (3)	0.3532 (4)	0.0938 (2)
C(71)	0.2512 (2)	0.5168 (3)	0.4010 (1)
C(72)	0.2160 (2)	0.5833 (3)	0.4370 (2)
C(73)	0.2299 (3)	0.5596 (4)	0.4955 (2)
C(74)	0.2798 (3)	0.4698 (5)	0.5191 (2)
C(75)	0.3148 (3)	0.4025 (4)	0.4844 (2)
C(76)	0.3007 (2)	0.4270 (3)	0.4252 (2)
C(81)	0.2417 (2)	0.7135 (3)	0.3251 (2)
C(82)	0.2999 (2)	0.7657 (3)	0.3675 (2)
C(83)	0.3098 (3)	0.8877 (4)	0.3711 (2)
C(84)	0.2621 (4)	0.9591 (4)	0.3322 (3)
C(85)	0.2074 (3)	0.9124 (4)	0.2899 (2)
C(86)	0.1958 (3)	0.7884 (4)	0.2853 (2)

[a] The estimated error in the last digit is given in parentheses. This form is used throughout. [b] The atom-numbering scheme is as shown in Figure A.[46]

Structural studies on the components of inorganic redox couples are, in their own right, of fundamental importance in inorganic chemistry. Such investigations detail the structural effects engendered by simple changes in the electronic configuration of the central metal and thus help elucidate the nature of the bonding forces within the overall complex.[15] Structural characterizations have been reported for many first-row transition-metal couples: e.g., Cr(III/II/I/0),[16] Fe(III/II),[17,18] Co(II/I),[19] Co(III/II),[20] Ni(III/II),[21] and Cu(II/I).[22-24] Similar characterizations of second-row Ru(III/II) couples have recently been the focus of considerable attention[25-29] for two related reasons. First, these couples are widely used in investigating the kinetics and mechanisms of electron-transfer reactions, and in these studies the effect

---

(8) Deutsch, E.; Glavan, K. A.; Sodd, V. J.; Nishiyama, H.; Ferguson, D. L.; Lukes, S. *J. Nucl. Med.* **1981**, *22*, 897.

(9) Deutsch, E.; Glavan, K. A.; Bushong, W.; Sodd, V. J. In *Applications of Nuclear Chemistry and Radiochemistry*; Lambrecht, R., Marcos, N., Eds.; Pergamon: New York, 1982; p 139.

(10) Gerson, M.; Deutch, E.; Nishiyama, H.; Libson, K.; Adolph, R.; Grossman, L.; Sodd, V.; Fortman, D.; Vanderheyden, J.-L.; Williams, C.; Saenger, E. *Eur. J. Nucl. Med.* **1983**, *8*, 371.

(11) Neves, M.; Libson, K.; Deutsch, E. In *Technetium in Chemistry and Nuclear Medicine*; Nicolini, M., Bandoli, G., Mazzi, U., Eds.; Cortina International: Verona, Italy, 1986; p 123.

(12) Neves, M.; Libson, K.; Deutsch, E. *Nucl. Med. Biol.* **1987**, *14*, 503.

(13) Vanderheyden, J.-L.; Heeg, M. J.; Deutsch, E. *Inorg. Chem.* **1985**, *24*, 1666.

(14) Deutsch, E.; Libson, K.; Vanderheyden, J.-L.; Ketring, A. R.; Maxon, H. R. *Nucl. Med. Biol.* **1986**, *13*, 465.

(15) Cotton, F. A.; Falvello, L. R.; Najjar, R. C. *Inorg. Chem.* **1983**, *22*, 770.

(16) Bohling, D. A.; Mann, K. R. *Inorg. Chem.* **1984**, *23*, 1426.

(17) (a) Beattie, J. K.; Moore, C. J. *Inorg. Chem.* **1982**, *21*, 1292. (b) Smith, D. A.; Heeg, M. J.; Heineman, W. R.; Elder, R. C. *J. Am. Chem. Soc.* **1984**, *106*, 3053.

(18) (a) Zalkin, A.; Templeton, D. H.; Ueki, T. *Inorg. Chem.* **1973**, *12*, 1641. (b) Baher, J.; Englehardt, L. M.; Figgis, B. N.; White, A. H. *J. Chem. Soc., Dalton Trans.* **1975**, 530. (c) Hair, N. J.; Beattie, J. K. *Inorg. Chem.* **1977**, *16*, 245. (d) Beattie, J. K.; Best, S. P.; Skelton, B. W.; White, A. H. *J. Chem. Soc., Dalton Trans.* **1981**, 2105. (e) Brunschwig, B. S.; Creutz, C.; McCartney, D. H.; Sham, T.-K.; Sutin, N. *Faraday Discuss. Chem. Soc.* **1982**, *74*, 113.

(19) Szalda, D. J.; Creutz, C.; Mahajan, D.; Sutin, N. *Inorg. Chem.* **1983**, *22*, 2372.

(20) Hammershoi, A.; Geselowitz, D.; Taube, H. *Inorg. Chem.* **1984**, *23*, 979.

(21) Szalda, D. J.; McCartney, D. H.; Sutin, N. *Inorg. Chem.* **1984**, *23*, 3473.

(22) Dagdigian, J. V.; McKee, V.; Reed, C. A. *Inorg. Chem.* **1982**, *21*, 1332.

(23) Diaddario, L. L., Jr.; Dockal, E. R.; Glick, M. D.; Ochrymowycz, L. A.; Rorabacher, D. B. *Inorg. Chem.* **1985**, *24*, 356.

(24) Bharadwaj, P. K.; Johm, E.; Xie, C.-L.; Zhang, D.; Hendrickson, D. N.; Potenza, J. A.; Schugar, H. J. *Inorg. Chem.* **1986**, *25*, 4541.

(25) Stynes, H. C.; Ibers, J. A. *Inorg. Chem.* **1971**, *10*, 2304.

(26) Bernhard, P.; Burgi, H.-B.; Hauser, J.; Lehmann, H.; Ludi, A. *Inorg. Chem.* **1982**, *21*, 3936.

(27) Richardson, E. D.; Walker, D. D.; Sutton, J. E.; Hodgson, K. O.; Taube, H. *Inorg. Chem.* **1979**, *18*, 2216.

(28) Gress, M. E.; Creutz, D.; Quicksall, C. O. *Inorg. Chem.* **1981**, *20*, 1522.

(29) Eggelston, D. S.; Goldsby, K. A.; Hodgson, D. J.; Meyer, T. J. *Inorg. Chem.* **1985**, *24*, 4573.

Table II. Fractional Atomic Positional Parameters of *trans*-$[Tc^{III}(DPPE)_2Cl_2]NO_3 \cdot HNO_3$[a]

atom	*x*	*y*	*z*
Tc	0.0000	0.0000	0.0000
Cl	0.23740 (6)	−0.00590 (6)	−0.08420 (4)
P(1)	0.05800 (6)	−0.14370 (5)	0.18620 (5)
P(2)	0.02650 (6)	−0.21960 (5)	−0.02870 (5)
N	0.2205 (3)	−0.5673 (2)	0.5006 (2)
O(1)	0.1853 (2)	−0.5342 (2)	0.5891 (2)
O(2)	0.1199 (2)	−0.5476 (2)	0.4472 (2)
O(3)	0.3433 (2)	−0.6186 (2)	0.4590 (2)
C(1)	0.0507 (2)	−0.3104 (2)	0.1956 (2)
C(2)	−0.0312 (2)	−0.3146 (2)	0.1123 (2)
C(11)	0.2269 (2)	−0.1856 (2)	0.2348 (2)
C(12)	0.2343 (3)	−0.2584 (2)	0.3446 (2)
C(13)	0.3622 (3)	−0.2971 (3)	0.3843 (2)
C(14)	0.4797 (3)	−0.2624 (3)	0.3166 (3)
C(15)	0.4726 (3)	−0.1904 (4)	0.2099 (3)
C(16)	0.3472 (3)	−0.1529 (3)	0.1677 (3)
C(21)	−0.0743 (2)	−0.0888 (2)	0.3050 (2)
C(22)	−0.0506 (3)	0.0003 (2)	0.3491 (2)
C(23)	−0.1515 (3)	0.0489 (3)	0.4363 (2)
C(24)	−0.2740 (3)	0.0092 (3)	0.4796 (2)
C(25)	−0.2979 (3)	−0.0787 (3)	0.4370 (2)
C(26)	−0.1985 (3)	−0.1263 (3)	0.3488 (2)
C(31)	−0.0800 (2)	−0.2393 (2)	−0.1141 (2)
C(32)	−0.2277 (3)	−0.1873 (3)	−0.0944 (2)
C(33)	−0.3102 (3)	−0.1978 (3)	−0.1610 (3)
C(34)	−0.2428 (3)	−0.2597 (3)	−0.2471 (2)
C(35)	−0.0971 (3)	−0.3121 (3)	−0.2673 (2)
C(36)	−0.0152 (3)	−0.3021 (3)	−0.2010 (2)
C(41)	0.2078 (2)	−0.3168 (2)	−0.0792 (2)
C(42)	0.2660 (3)	−0.4496 (3)	−0.0291 (2)
C(43)	0.3971 (4)	−0.5221 (3)	−0.0774 (3)
C(44)	0.4708 (3)	−0.4655 (3)	−0.1781 (3)
C(45)	0.4151 (3)	−0.3332 (3)	−0.2298 (2)
C(46)	0.2854 (2)	−0.2598 (2)	−0.1794 (2)
H(1)	0.0	0.5000	0.5000

[a] The atom-numbering scheme is as shown in Figures B[46] and C.[46]

Table III. Selected Bond Lengths (Å) and Angles (deg) for *trans*-$[Tc^{II}(DPPE)_2Cl_2]$ and *trans*-$[Tc^{III}(DPPE)_2Cl_2]^+$

	Tc(II)	Tc(III)[a]
	Bond Lengths	
Tc–Cl(1)	2.410 (1)	2.319 (1)[b]
Tc–Cl(2)	2.438 (1)	
Tc–P(1)	2.444 (1)	2.509 (1)[c]
Tc–P(3)	2.417 (1)	
Tc–P(2)	2.444 (1)	2.492 (1)[d]
Tc–P(4)	2.410 (1)	
	Bond Angles	
Cl(1)–Tc–Cl(2)	173.5 (1)	180[a]
Cl(1)–Tc–P(1)	81.41 (3)	94.98 (2)[e]
Cl(1)–Tc–P(3)	92.92 (3)	
Cl(2)–Tc–P(1)	101.03 (3)	
Cl(2)–Tc–P(3)	84.65 (3)	
Cl(1)–Tc–P(2)	88.24 (3)	93.69 (2)[f]
Cl(1)–Tc–P(4)	90.14 (3)	
Cl(2)–Tc–P(2)	98.10 (3)	
Cl(2)–Tc–P(4)	83.51 (3)	
P(1)–Tc–P(2)	79.68 (3)	80.57 (3)[g]
P(3)–Tc–P(4)	79.54 (3)	

[a] Centrosymmetric complex. [b] Tc–Cl. [c] Tc–P(1). [d] Tc–P(2). [e] Cl–Tc–P(1). [f] Cl–Tc–P(2). [g] P(1)–Tc–P(2).

Table IV. Derived Second-Order Rate Constants[a] Governing the Reaction of *trans*-$[Tc^{II}(DPPE)_2X_2]$ (X = Cl, Br) with $[(en)_2Co(S(CH_2C_6H_4CH_3)CH_2CH_2NH_2)]^{3+}$

solvent	μ, M	$10^{-4}k_2$, $M^{-1}\ s^{-1}$[b]	*n*[c]
	X = Cl		
CH_3CN	0.10	3.0 (7)	6[d]
CH_3CN	0.08	4.2 (3)	2[e]
CH_3CN	0.05	2.5 (3)	2
0.5% H_2O/CH_3CN	0.10	1.6 (1)	1
1.8% DMF/CH_3CN	0.10	0.68 (4)	3
DMF	0.10	0.0037 (7)	1
	X = Br		
CH_3CN	0.10	1.2 (3)	8
CH_3CN	0.05	1.3 (3)	3
CH_3CN	0.025	1.2 (2)	1
CH_3CN	0.005	2.5 (2)	1
0.5% H_2O/CH_3CN	0.10	0.67 (2)	1
2.5% H_2O/CH_3CN	0.10	0.31 (1)	1

[a] Conditions (unless otherwise noted): 25 °C, ionic strength maintained with tetrabutylammonium perchlorate. [b] The standard deviation of the last digit is given in parentheses. [c] Number of independent data sets. [d] Two out of six data sets obtained with tetraethylammonium perchlorate to maintain ionic strength. [e] Ionic strength maintained with tetraethylammonium perchlorate.

Table V. Qualitative Rate Data Describing Outer-Sphere Electron-Transfer Reactions of *trans*-$[Tc^{II}(DPPE)_2Cl_2]$[a]

oxidant	solvent	k_2, $M^{-1}\ s^{-1}$
A_6Ru^{3+}	DMF	<10
	5% DMF/CH_3CN	$>10^7$
ferrocenium	10% DMF/CH_3CN	$>10^7$
$A_5CoOH_2^{3+}$	10% DMF/CH_3CN	140
	5% DMF/CH_3CN	310
A_6Co^{3+}	10% DMF/CH_3CN	<10
$A_5CoCl_2^+$	10% DMF/CH_3CN	<10
A_5CoBr^{2+}	10% DMF/CH_3CN	300
$(en)_2Co(SCH_2CH_2NH_2)^{2+}$	40% DMF/CH_3CN	$>10^7$

[a] Conditions: 25 °C, μ = 0.10 M maintained with tetrabutylammonium perchlorate.

Table VI. Average Metal–Ligand Bond Lengths (Å) in Tc(III/II) and Ru(III/II) Complexes

	M^{III}	M^{II}	Δd[a]	ref
trans-$[Tc(DPPE)_2Cl_2]^{+/0}$				
Tc–Cl	2.424 (1)	2.319 (1)	0.105 (2)	*b*
Tc–P	2.428 (1)	2.500 (1)	−0.072 (2)	*b*
cis-$[Ru(bpy)_2Cl_2]^{+/0}$				
Ru–Cl	2.426 (1)	2.325 (3)	0.101 (3)	29
Ru–N_c(bpy)[c]	2.013 (2)	2.050 (7)	−0.037 (8)	29
Ru–N_t(bpy)[c]	2.054 (2)	2.060 (7)	−0.006 (8)	29
$[A_5Ru(pyz)]^{3+/2+}$				
Ru–pyz	2.006 (6)	2.076 (8)	−0.070 (10)	28
cis-$[A_4Ru(isn)_2]^{3+/2+}$				
Ru–isn	2.099 (4)	2.060 (4)	−0.039 (6)	27

[a] $d(M^{II}-L) - d(M^{III}-L)$. [b] This work. [c] N_c refers to bpy nitrogen atoms that are cis to other bpy nitrogen atoms and trans to Cl. N_t refers to bpy nitrogen atoms that are trans to other bpy nitrogen atoms and cis to Cl.

of reorganizing the inner coordination sphere of the ruthenium center on the rate of electron transfer can be calculated from the equilibrium bond lengths of the components of the Ru(III/II) couple.[19,21,26-31] Second, when the components of these couples contain ligands of different π-acidities, the effect of oxidation state on π-bonding can be probed directly.[27-29] This paper extends these structural and kinetic concepts to the adjacent second-row element technetium by means of the title Tc(III/II) complexes. A related study, involving the Tc(II/I) couple $[Tc(DMPE)_3]^{2+/+}$, has recently been reported,[32] although in this earlier case it was not possible to obtain single-crystal X-ray structural data for both components of the Tc(II/I) redox pair. The wide range of low-valent, redox-active, substitution-inert technetium complexes that are available[5,6] makes it likely that the systematic study of these species will contribute substantially to the elucidation of π-bonding effects and to the detailed description of electron-transfer processes.[32]

---

(30) Newton, M. D.; Sutin, N. *Annu. Rev. Phys. Chem.* **1984**, *35*, 437.

(31) Sutin, N. *Prog. Inorg. Chem.* **1983**, *30*, 441.

(32) Doyle, M. N.; Libson, K.; Woods, M.; Sullivan, J. C.; Deutsch, E. *Inorg. Chem.* **1986**, *25*, 3367.

Acronyms and Abbreviations

A = ammonia
D = chelating bis(tertiary arsine or phosphine)
X = halide or pseudohalide
en = ethylenediamine
bpy = 2,2′-bipyridine
isn = isonicotinamide
pyz = pyrazine
DMF = *N*,*N*-dimethylformamide
DPPE = 1,2-bis(diphenylphosphino)ethane
DMPE = 1,2-bis(dimethylphosphino)ethane
diars = *o*-phenylenebis(dimethylarsine)

Experimental Section

Caution! Technetium-99 emits a low-energy (0.292-MeV) β-particle with a half-life of 2.12×10^5 years. When this material is handled in milligram amounts, it does not present a serious health hazard since common laboratory materials provide adequate shielding. Bremsstrahlung is not a significant problem due to the low energy of the β-particle emission, but normal radiation safety procedures must be used at all times to prevent contamination and inadvertent ingestion or inhalation of this isotope.

Materials. Unless otherwise specified, the symbol Tc refers to the technetium isotope of mass 99. This isotope was purchased from Oak Ridge National Laboratory in the form of solid ammonium pertechnetate, which was then purified as previously described.[33]

Unless otherwise noted, all chemicals were of reagent grade. Solvents used in the kinetic studies were of HPLC grade, or equivalent. Tetraethylammonium perchlorate and tetrabutylammonium perchlorate were of polarographic grade. Solutions of ferrocenium perchlorate were prepared by PbO_2 oxidation of ferrocene solutions. Triply recrystallized perchlorate salts of $[(en)_2Co(SCH_2CH_2NH_2)]^{2+}$ and $[(en)_2Co(S(CH_2C_6H_4CH_3)CH_2CH_2NH_2)]^{3+}$ and the triply recrystallized trifluoromethanesulfonate salt of $[(NH_3)_6Ru]^{3+}$ were available from previous studies.[34–36] Perchlorate salts of $[(NH_3)_6Co]^{3+}$, $[(NH_3)_5Co(H_2O)]^{3+}$, $[(NH_3)_5CoCl]^{2+}$, and $[(NH_3)_5CoBr]^{2+}$ were prepared and purified according to literature procedures.[37]

The Tc(III) complexes *trans*-$[Tc(DPPE)_2Cl_2]Cl$ and *trans*-$[Tc(DPPE)_2Br_2]Br$ were prepared and purified as previously described.[33] The Tc(II) complex *trans*-$[Tc(DPPE)_2Cl_2]$, used in the crystallographic study, was prepared by reduction of the Tc(III) analogue as previously described.[33] For the kinetic studies the *trans*-$[Tc^{II}(DPPE)_2X_2]$ (X = Cl, Br) complexes were prepared by the following procedure. Fifty milligrams of red-orange *trans*-$[Tc^{III}(DPPE)_2X_2]X$[33] was dissolved in 20–30 mL of absolute ethanol, and 1 mL of neat ethanethiol was added. The desired yellow Tc(II) product precipitates from this reaction mixture after several minutes at room temperature. The precipitate was removed by filtration, washed several times with absolute ethanol, and then dried under a stream of inert gas. The spectrophotometric and electrochemical properties of the Tc(II) complexes prepared in this manner agree with those previously reported.[33]

Kinetics. The stopped-flow instrumentation and general techniques used in the kinetic studies have been previously described.[32] Reactions were conducted at 25 °C in nonaqueous solvents (acetonitrile, *N*,*N*-dimethylformamide, or mixtures of these) with a tetraalkylammonium perchlorate supporting electrolyte. Most reactions were conducted at ionic strength 0.10 ± 0.01 M. All of the supporting electrolyte was added to the oxidant solution, since in the presence of 0.10 M tetraalkylammonium perchlorate the *trans*$[Tc^{II}(DPPE)_2X_2]$ complexes are oxidized to the Tc(III) analogues in about 10 min. Reactions were conducted with a pseudo-first-order excess of oxidant, and the Tc(II) reductant was usually present at ca. 2×10^{-5} M. The rate of reaction was determined by monitoring the appearance of the Tc(III) product at the characteristic absorption maximum of this species (480 nm for *trans*-$[Tc(DPPE)_2Cl_2]^+$ and 504 nm for *trans*-$[Tc(DPPE)_2Br_2]^+$[33]). All absorbance vs time data were adequately described by first-order kinetics and were analyzed by standard nonlinear least-squares techniques to yield values of k_{obsd}:

$$d\{\ln [Tc(III)]\}/dt = k_{obsd}$$

For $[(en)_2Co(S(CH_2C_6H_4CH_3)CH_2CH_2NH_2)]^{3+}$ as oxidant, sufficient data were obtained to show that k_{obsd} is linearly dependent on the concentration of oxidant

$$k_{obsd} = k_2[\text{oxidant}]$$

and k_2 values were obtained by linear least-squares analysis of k_{obsd} vs [Co(III)] data. This second-order rate law was assumed to hold for the other oxidants investigated, and in these cases the quoted k_2 values were obtained by averaging k_2 values obtained in replicate experiments. All quoted errors are standard deviations.

X-ray Characterization of *trans*-$[Tc^{II}(DPPE)_2Cl_2]$. A yellow crystal of approximate dimensions 0.34 × 0.20 × 0.22 mm was mounted on a glass fiber, with the fiber nearly parallel to the long axis of the crystal. CuKα radiation was used to obtain *h*0*l*, *hk*0, *h*1*l*, and *hk*1 precession photographs. Systematic absences for *h*0*l*, *h* odd, and for 0*k*0, *k* odd, indicated the monoclinic space group $P2_1/a$ (nonstandard setting[38] of $P2_1/c$, No. 14, C_{2h}^5) with approximate cell constants a = 17.74 (3) Å, b = 11.27 (3) Å, c = 23.19 (3) Å, and β = 103.3 (3)°. This crystal was optically centered on a Syntex P$\bar{1}$ diffractometer equipped with a graphite monochromator and a molybdenum target tube (λ = 0.710 73 Å), and a full rotation photograph was obtained. Fifteen intense reflections were chosen and centered by using manufacturer-supplied software. The autoindexing program gave axial choices in agreement with those previously determined from precession photographs. Oscillation photographs (±14°) were taken about each of these axes to check crystal quality and to ensure correctness of indexing. Precise cell constants were determined by least-squares refinement[39] of 15 paired reflections measured at $\pm 2\theta$ in the range |12.1 – 21.9°|: a = 17.821 (4) Å, b = 11.187 (2) Å, c = 23.572 (4) Å, β = 103.55 (1)°, and Z = 4. The density calculated from these data is 1.42 g cm^{-3}; the measured density is 1.39 (3) g cm^{-3} (neutral buoyancy, carbon tetrachloride/diethyl ether). All measurements were performed at room temperature.

Intensity measurements were made as previously described[40] for 7048 reflections with $2\theta \leq 2\sigma(I)$, where p, the ignorance factor used to calculate[40] $\sigma(I)$, was set equal to 0.025. The θ–2θ scans for these measurements were 1.2° wide. Scan rates varied from 2.0 to 8.0° min^{-1} depending on the intensity of the reflection. Four standard reflections, which were remeasured every 40 reflections, were used to check instrument and crystal stability and to account for long-term drift. The drift corrections varied in a random manner from 0.973 to 1.006. Absorption corrections were applied with the value of μ = 6.06 cm^{-1}.

Structure Solution and Refinement of *trans*-$[Tc^{II}(DPPE)_2Cl_2]$. A Patterson vector map[41] indicated positions for the technetium, chlorine, and phosphorus atoms. A corresponding electron density map clearly showed the positions of all remaining non-hydrogen atoms. Least-squares refinement of the model using atom positions, general scale factor, anisotropic thermal parameters and file weights converged to R_1 = 0.034 and R_2 = 0.029.[42] The hydrogen atoms were placed at their calculated positions (C–H = 0.97 Å) and were not refined. The 4945 values of F_o were used to refine 532 variables. In the final cycle of refinement the maximum shift per error was 0.15 and the average shift per error was 0.027. The largest peak on a final difference electron density map, 0.23 e Å^{-3}, was located about 0.8 Å from the Tc atom. Zerovalent scattering curves were taken from standard tabulations for Tc, Cl, P, and C[43] and H.[44] Corrections for anomalous dispersion[45] were made by using $\Delta f'$ and $\Delta f''$ values of –1.590 and 0.759 for Tc, 0.132 and 0.159 for Cl, 0.090 and 0.095 for P, and 0.002 and 0.002 for C. The values of F_o and F_c are given in Table A.[46]

X-ray Characterization of *trans*-$[Tc^{III}(DPPE)_2Cl_2]NO_3\cdot HNO_3$. A red crystal of approximate dimensions 0.81 × 0.80 × 0.50 mm was mounted on a glass fiber. CuKα radiation was used to obtain 0*kl*, *hk*0, 1*kl*, and

---

(33) Libson, K.; Deutsch, E.; Barnett, B. *Inorg. Chem.* **1983**, *22*, 1695.
(34) Lavallee, D. K.; Lavallee, C.; Sullivan, J. C.; Deutsch, E. *Inorg. Chem.* **1973**, *12*, 570.
(35) Asher, L. E.; Deutsch, E. *Inorg. Chem.* **1973**, *12*, 1774.
(36) Kennard, G. J.; Deutsch, E. *Inorg. Chem.* **1978**, *17*, 2225.
(37) Schlessinger, G. G. *Inorganic Laboratory Preparations*; Chemical Publishing: New York, 1962; pp 206–222.
(38) *International Tables for X-ray Crystallography*, 2nd ed.; Kynoch: Birmingham, England, 1976; Vol. 1.
(39) Santoro, A.; Mighell, A. D. *Acta Crystallogr., Sect. A: Cryst. Phys., Diffr., Theor. Gen. Crystallogr.* **1976**, *A26*, 124.
(40) Elder, R. C.; Florian, L. R.; Lake, R. E.; Yacynych, A. M. *Inorg. Chem.* **1973**, *12*, 2690.
(41) All computations were performed by using a local version of X-RAY 67: Stewart, J. M. "Crystallographic Computer System"; University of Maryland: College Park, MD, 1967.
(42) $R_1 = \sum||F_o| - |F_c||/\sum|F_o|$; $R_2 = [\sum w(|F_o - F_c|)^2/\sum w(F_o)^2]^{1/2}$.
(43) Cromer, D. T.; Mann, J. B. *Acta Crystallogr., Sect. A: Cryst. Phys., Diffr., Theor. Gen. Crystallogr.* **1968**, *A24*, 321.
(44) Stewart, R. F.; Davidson, E. R.; Simpson, W. T. *J. Chem. Phys.* **1965**, *42*, 3175.
(45) *International Tables for X-ray Crystallography*; Kynoch: Birmingham, England, 1974; Vol. 4, pp 148–150.
(46) All tables and figures designated by alphabetic characters have been deposited as supplementary material.

*hk*1 precession photographs, which indicated a triclinic crystal with approximate cell constants a = 10.09 (2) Å, b = 11.12 (2) Å, c = 12.81 (4) Å, α = 71.83 (4)°, β = 73.65 (4)°, and γ = 69.45 (4)°. This crystal was optically centered on the diffractometer, and the procedures noted above were employed to check crystal quality. Least-squares refinement[39] of 15 intense reflections measured at both $\pm 2\theta$ values in the range of $|16.6 - 26.2°|$ gave the following lattice constants: a = 10.083 (2) Å, b = 11.119 (4) Å, c = 12.767 (1) Å, α = 71.80 (1)°, β = 73.68 (1)°, γ = 69.35(1)°, and Z = 1. The calculated density is 1.44 g cm^{-3}; the measured density is 1.45 (3) g cm^{-3} (neutral buoyancy, carbon tetrachloride/diethyl ether). All measurements were performed at room temperature.

The data collection was carried out as described above with the following differences: intensity data, maximum $2\theta < 58°$; number of reflections 7140 (measured), 6627 (unique), 5697 ($I \geq 2\sigma(I)$); ignorance factor P = 0.030; θ–2θ scans, 1.6° wide; scan rate 3.0–8.0° min^{-1}; random drift corrections from 0.985 to 1.058; linear absorption coefficient μ = 5.61 cm^{-1}.

Structure Solution and Refinement of *trans*-$[Tc^{III}(DPPE)_2Cl_2]NO_3\cdot HNO_3$. A Patterson vector map[41] indicated positions for the technetium, chlorine, and phosphorus atoms. A corresponding electron density map clearly showed the positions of all remaining non-hydrogen atoms. The hydrogen atom in the anion $O_3N\cdot HNO_3^-$ was located by using a difference electron density map. Least-squares refinement of the model using atom positions, general scale factor, anisotropic thermal parameters, and file weights converged to R_1 = 0.038 and R_2 = 0.035.[42] All hydrogen atoms except that in the anion were placed at their calculated positions (C–H = 0.97 Å) and were not refined. The 5697 values of F_o were used to refine 304 variables. In the final cycle of refinement the maximum shift per error was 0.047 and the average shift per error was 0.011. The largest peak on a final difference electron density map, 0.37 e $Å^{-3}$, was located about 1.0 Å from the Tc atom. Scattering curves were taken from standard tabulations for Tc, Cl, P, O, N, and C[43] and H.[44] Corrections for anomalous dispersion[45] were made by using $\Delta f'$ and $\Delta f''$ values of −1.590 and 0.759 for Tc, 0.132 and 0.159 for Cl, 0.090 and 0.095 for P, 0.008 and 0.006 for O, 0.004 and 0.003 for N, and 0.002 and 0.002 for C. The values of F_o and F_c are given in Table B.[46]

Results

Crystal Structures of Tc(II) and Tc(III) Complexes. Final fractional atomic positional parameters and their estimated standard deviations are given in Tables I and II for the Tc(II) and Tc(III) complexes, respectively. The corresponding anisotropic thermal parameters may be found in Tables C and D.[46] Figure 1 shows the associated ellipsoids for the Tc(II) complex, without atom labels; the analogous figure of the Tc(III) complex is essentially identical. Figures A[46] and B[46] show respectively the associated ellipsoids for the Tc(II) and Tc(III) complexes along with the atom-labeling schemes. Figure C[46] shows the $H(NO_3)_2^-$ anion of the Tc(III) salt. Selected bond lengths and bond angles for the two complexes are given in Table III, while complete listings of these parameters are in Tables E–H.[46] Tables I[46] and J[46] list the calculated hydrogen atom positions for the two complexes.

Both the Tc(II) and the Tc(III) complexes are six-coordinate with an approximately octahedral coordination environment. The donor phosphorus atoms of the two DPPE ligands occupy the four equatorial coordination sites, forming two five-membered rings, while the two chloride ligands occupy mutually trans positions. This trans octahedral geometry is typical for Tc(III) cations of the general formula $[TcD_2X_2]^+$.[33,47,48]

The site symmetry of the Tc(III) cation forces this complex to be centrosymmetric with no significant distortions from D_{2h} symmetry. The neutral Tc(II) complex has no such restrictions, and significant distortions are observed in the geometry of the first coordination sphere (Table III). The Tc–Cl distances differ by about 0.03 Å, while the Tc–P distances to one DPPE ligand (P(1), P(2)) differ from the distances to the other DPPE ligand (P(3), P(4)) by about this same amount. Inner coordination sphere bond length differences of this magnitude, and larger, have been observed in the related *trans*-$[Tc^{III}(diars)_2Cl_2]X$ complexes[47] (X = Cl^-, ClO_4^-) and can be reasonably ascribed to the effects of lattice packing forces.

Kinetics. Observed pseudo-first-order rate constants, k_{obsd}, governing the reduction of $[(en)_2Co(S(CH_2C_6H_4CH_3)CH_2CH_2NH_2)]^{3+}$ by the Tc(II) complexes *trans*-$[Tc(DPPE)_2X_2]$ (X = Cl, Br), as a function of [Co], ionic strength, and solvent composition, are given in Tables K[46] and L.[46] The second-order rate parameters calculated from these results are given in Table IV. Qualitative results on the rate of *trans*-$[Tc(DPPE)_2Cl_2]$ reduction of a variety of oxidants are summarized in Table V.

Discussion

Single-Crystal X-ray Structures. The trans octahedral geometries observed for the title Tc(II) and Tc(III) DPPE complexes are entirely as expected on the basis of previously reported structures of *trans*-$[Tc^{II}(DPPE)_2(NCS)_2]$[49] and *trans*-$[Tc^{III}(DPPE)_2Br_2]^+$.[33] Trans octahedral structures have also been reported for the related Tc(III) cations *trans*-$[Tc(DMPE)_2Cl_2]^+$[48] and *trans*-$[Tc(diars)_2Cl_2]^+$,[47] and in fact this is the most commonly observed geometry for $[MD_2X_2]^{n+}$ species.[50,51]

The average Tc^{III}–Cl, Tc^{III}–P, and Tc^{II}–P bond lengths observed in the title structures (Table VI) are in good agreement with previously reported values for these parameters. The average Tc^{III}–Cl bond length of 2.319 (1) Å (Table VI) can be directly compared to Tc^{III}–Cl lengths of 2.323 (3), 2.329 (1), and 2.318 (6) Å observed in *trans*-$[Tc(DMPE)_2Cl_2]^+$[48] and two salts of *trans*-$[Tc(diars)_2Cl_2]^+$.[47] The average Tc^{III}–P bond length of 2.500 (1) Å (Table VI) is identical with the 2.50 (1) Å Tc^{III}–P length of *trans*-$[Tc(DPPE)_2Br_2]^+$.[33] The Tc^{III}–P lengths within both of the DPPE complexes are somewhat longer than the Tc^{III}–P length (2.44 (1) Å) within the DMPE complex *trans*-$[Tc(DMPE)_2Cl_2]^+$,[48] presumably because the methyl groups of DMPE generate less interligand repulsion than do the larger phenyl groups of DPPE. The average Tc^{II}–P bond length observed in *trans*-$[Tc(DPPE)_2Cl_2]$ (2.428 Å; Table VI) is in good agreement with the 2.44 (1) Å Tc^{II}–P bond length reported for *trans*-$[Tc(DPPE)_2(NCS)_2]$.[49]

The differences in bond lengths observed for the pair of related Tc(III/II) complexes *trans*-$[Tc(DPPE)_2Cl_2]^{+/0}$ are summarized in Table VI. This table also presents comparable data for the pair of related Ru(III/II) complexes *cis*-$[Ru(bpy)_2Cl_2]^{+/0}$[29] and selected data for the higher charged Ru(III/II) complexes $[RuA_5(pyz)]^{3+/2+}$[28] and $[RuA_4(isn)_2]^{3+/2+}$.[27] Oxidation of the metal center from Tc(II) to Tc(III) causes the Tc–Cl bond length to *shorten* by 0.105 (2) Å, as expected for a ligand that binds primarily through ionic interactions. An identical shortening of the Ru–Cl bond length is observed upon oxidation of Ru(II) to Ru(III), supporting the description of chloride as a ligand that binds primarily through σ-donation. In dramatic contrast to the behavior of the Tc–Cl linkage, the Tc–P bond *lengthens* by 0.072 (2) Å upon oxidation of Tc(II) to Tc(III). This effect is readily understood on the basis that the Tc–P interaction is primarily covalent. π-back-bonding from Tc to P is favored when the Tc center has a lower formal charge, and thus, the Tc–P bond lengthens when the oxidation state of the metal increases.[32,48] Similar, but decidedly smaller, effects are observed in the Ru–N bond lengths of *cis*-$[Ru(bpy)_2Cl_2]^{+/0}$ since the Ru–bpy bonding interactions also have a large covalent component. The restraints of the bpy chelate ring appear to restrict expression of this π-bonding effect; a Ru(III/II) complex containing the monodentate π-acid pyrazine ligand exhibits bond length changes of the same magnitude observed for the Tc–P bond (Table VI).

Structural Contribution to Self-Exchange Rate. Current theory allows the inner-sphere reorganization barrier to the rate of self-exchange of a redox couple to be estimated from crystallo-

---

(47) Elder, R. C.; Whittle, R.; Glavan, K. A.; Johnson, J. F.; Deutsch, E. *Acta Crystallogr., Sect. B: Struct. Crystallogr. Cryst. Chem.* **1980**, *B36*, 1662.

(48) Vanderheyden, J.-L.; Ketring, A. R.; Libson, K.; Heeg, M. J.; Roecker, L.; Motz, P.; Whittle, R.; Elder, R. C.; Deutsch, E. *Inorg. Chem.* **1984**, *23*, 3184.

(49) Bandoli, G.; Mazzi, U.; Ichimura, A.; Libson, K.; Heineman, W. R.; Deutsch, E. *Inorg. Chem.* **1984**, *23*, 2898.

(50) McAuliffe, C. A., Ed. *Transition Metal Complexes of Phosphorus, Arsenic and Antimony Ligands*; Wiley: New York, 1973.

(51) McAuliffe, C. A.; Levason, W. *Phosphine, Arsine and Stibine Complexes of the Transition Elements*; Elsevier: New York, 1979.

graphically derived metal–ligand bond distances.[19,21,26–32] The relevant expression is

$$\Delta G_{\text{in}}^{*} = 3\bar{f}(\Delta d)^2/2$$

where $\bar{f}$ is the reduced force constant describing vibration of the metal–ligand bond. The strong dependence of ΔG_{in}^{*} on Δd, the change in bond length engendered by the electron-transfer process, has previously been documented for $[\mathrm{M(bpy)_3}]^{n+}$ systems.[19,21] The bond length changes observed in the *trans*-$[\mathrm{Tc(DPPE)_2Cl_2}]^{+/0}$ couple (Table VI) are relatively small, as expected for a spin-paired d^4/d^5 system that does not undergo a change in the number of σ d electrons during electron transfer.[18e,21,32] The weighted average of Tc–Cl and Tc–P bond length changes is calculated to be 0.084 Å by means of the expression

$$\Delta d = \left[\frac{2(\Delta d_{\text{Tc–Cl}})^2 + 4(\Delta d_{\text{Tc–P}})^2}{6}\right]^{1/2}$$

This is slightly larger than the 0.068 Å Tc–P bond length change observed in the $[\mathrm{Tc(DMPE)_3}]^{2+/+}$ couple,[32] and thus the calculated value of ΔG_{in}^{*} for the *trans*-$[\mathrm{Tc(DPPE)_2Cl_2}]^{+/0}$ couple is slightly larger than that calculated for the $[\mathrm{Tc(DMPE)_3}]^{2+/+}$ couple (2.6 vs 1.7 kcal/mol). The value of $\bar{f}$ for the Tc–Cl and Tc–P stretches in both calculations is estimated from the known symmetrical Tc–Cl stretching frequency of $[\mathrm{TcCl_6}]^{2-}$.[32] The relatively small value of ΔG_{in}^{*} calculated for the *trans*-$[\mathrm{Tc(DPPE)_2Cl_2}]^{+/0}$ couple implies that Tc(III/II) couples of the general formula *trans*-$[\mathrm{TcD_2X_2}]^{+/0}$ should provide kinetically reactive redox partners.

Kinetics. The components of the *trans*-$[\mathrm{Tc(DPPE)_2Cl_2}]^{+/0}$ couple are essentially insoluble in water, and thus kinetic studies involving these complexes are limited to nonaqueous solvents. Electron-transfer studies in nonaqueous solvents are plagued by a variety of experimental and theoretical problems,[52–55] which have deterred the acquisition of a large data base of kinetic parameters. Among other complicating factors, the rate of outer-sphere electron transfer is very sensitive to the nature of the nonaqueous solvent and there is no standard set of conditions for acquisition of new kinetic data.

In a series of preliminary experiments (Table V), it was determined that *trans*-$[\mathrm{Tc^{II}(DPPE)_2Cl_2}]$ is a facile reductant for $[\mathrm{A_6Ru}]^{3+}$, an outer-sphere oxidant that has a low inner-sphere reorganizational barrier, but that the rate is much faster in acetonitrile than it is in DMF. In fact, when the DMF/$\mathrm{CH_3CN}$ ratio is increased, the rate of this reaction can be decreased from one that is too fast to measure on the stopped-flow spectrophotometer to one that does not proceed detectably within several minutes. Reductions of other facile oxidants such as ferrocennium[52,55] and $[\mathrm{(en)_2Co(SCH_2CH_2NH_2)}]^{2+}$[56] also proceed rapidly, whereas reductions of sluggish oxidants such as $[\mathrm{A_5CoOH_2}]^{3+}$, $[\mathrm{A_5CoBr}]^{2+}$, and $[\mathrm{(en)_2Co(S(CH_2C_6H_4CH_3)CH_2CH_2NH_2)}]^{3+}$[36] proceed at intermediate rates, which can be conveniently monitored, and the last system was chosen for more detailed study.

The data of Table IV show that the rate of *trans*-$[\mathrm{Tc^{II}(DPPE)_2X_2}]$ (X = Cl, Br) reduction of $[\mathrm{(en)_2Co(S(CH_2C_6H_4CH_3)CH_2CH_2NH_2)}]^{3+}$ is markedly dependent on the composition of the solvent. The addition of small amounts of either water or DMF to the acetonitrile solvent detectably retards the rate of reduction. Changing the solvent from neat acetonitrile to neat DMF slows the *trans*-$[\mathrm{Tc^{II}(DPPE)_2Cl_2}]$ reduction rate by almost 4 orders of magnitude. However, the rate of reduction is relatively independent of ionic strength (and of the nature of the supporting electrolyte), as might be expected for the reaction of an uncharged species.

At 0.10 M ionic strength, where most data are available, the *trans*-$[\mathrm{Tc^{II}(DPPE)_2Cl_2}]$ complex reacts about a factor of 2.5 faster than the Br analogue. This ordering of rates is qualitatively consistent with the fact that the Cl complex is a better reductant than is the Br analogue.[33] However, this observed ratio of rates is only about one-third the ratio expected from the fact that the difference in reduction potentials between the two complexes is about 0.10 V.[33] The origins of this relatively low rate ratio will have to be determined by further studies in these nonaqueous media.

The salient result of these kinetic studies is that the *trans*-$[\mathrm{Tc^{II}(DPPE)_2X_2}]$ (X = Cl, Br) complexes are relatively facile reductants in nonaqueous media, consistent with expectations derived from X-ray structural characterizations of the title complexes.

Acknowledgment. Financial support was provided in part by the National Institutes of Health, Grant No. HL-21276, GM-35404, and CA-42179. A portion of this work was performed under the auspices of the Office of Basic Energy Sciences, Division of Chemical Sciences, U.S. Department of Energy, under Contract No. W-31-109-ENG-38.

Registry No. *trans*-$[\mathrm{Tc^{II}(DPPE)_2Cl_2}]$, 93293-97-1; *trans*-$[\mathrm{Tc^{III}(DPPE)_2Cl_2]NO_3\cdot HNO_3}$, 116126-26-2; *trans*-$[\mathrm{Tc^{II}(DPPE)_2Br_2}]$, 111070-90-7; $[\mathrm{(en)_2Co(S(CH_2C_6H_4CH_3)CH_2CH_2NH_2)}]^{3+}$, 65622-77-7.

Supplementary Material Available: Tables C–J, showing anisotropic thermal parameters and bond lengths and angles for both *trans*-$[\mathrm{Tc^{II}(DPPE)_2Cl_2}]$ and *trans*-$[\mathrm{Tc^{III}(DPPE)_2Cl_2]NO_3\cdot HNO_3}$, Tables K and L, giving observed pseudo-first-order rate parameters, and Figures A–C, showing perspective drawings of *trans*-$[\mathrm{Tc(DPPE)_2Cl_2}]$, *trans*-$[\mathrm{Tc(DPPE)_2Cl_2}]^{+}$, and $[\mathrm{H(NO_3)_2}]^{-}$ (18 pages); Tables A and B, giving F_c and F_o values for *trans*-$[\mathrm{Tc^{II}(DPPE)_2Cl_2}]$ and *trans*-$[\mathrm{Tc^{III}(DPPE)_2Cl_2]NO_3\cdot HNO_3}$ (41 pages). Ordering information is given on any current masthead page.

---

(52) Borchardt, D.; Wherland, S. *Inorg. Chem.* **1986**, *25*, 901.

(53) Nielson, R. M.; Wherland, S. *Inorg. Chem.* **1986**, *25*, 2437.

(54) Nielson, R. M.; Wherland, S. *Inorg. Chem.* **1984**, *23*, 1338.

(55) Borchardt, D.; Wherland, S. *Inorg. Chem.* **1984**, *23*, 2537.

(56) Deutsch, E.; Root, M. J.; Nosco, D. L. In *Advances in Inorganic and Bioinorganic Mechanisms*; Sykes, A. G., Ed.; Academic: New York, 1982; Vol. 1, p 269.